BMC Plant Biology

RESEARCH

Open Access

Transcriptome profiling reveals the mechanism of fruit navel development in melon (*Cucumis melo* L.)

Tiantian Ren[1], Xuqian Shi[1], Shuxin Zhou[1], Kanghui Fan[1], Rui Zhang[1], Lanchun Nie[1,2,3] and Wensheng Zhao[1,2*]

Abstract

Background Melon is an important horticultural crop cultivated extensively worldwide. The size of the fruit navel, the terminal region of melon fruits, significantly influences the appearance quality of the fruit. However, the regulatory factors and molecular mechanisms governing the fruit navel development remain poorly understood in melon.

Results In this study, the regulators and mechanisms underlying fruit navel development were investigated through phenotypic analysis, RNA sequencing (RNA-seq) and RT-qPCR methods. The inbred line 'T03' and a big fruit navel mutant 'BFN' of melon were used as experimental materials. RNA-seq analysis identified 116 differentially expressed genes (DEGs), including 54 up-regulated and 62 down-regulated genes, in both the green bud (GB) and ovary at anthesis (OA) stages of the 'BFN' melon compared to the 'T03' melon. Functional enrichment analysis revealed that these 116 DEGs were significantly associated with "Sesquiterpenoid and triterpenoid biosynthesis", "Circadian rhythm—plant", "Galactose metabolism" and "Biosynthesis of various alkaloids" pathways. There were three (AP2/ERF, MYB and C2H2 types) and eight (AP2/ERF, MADS-box, homeobox domain and bZIP types) transcription factors presented in up-regulated and down-regulated DEGs, and their putative target genes were predicted. Based on KEGG and expression analyses, two terpene cyclase/mutase genes (*MELO3 C001812* and *MELO3 C004329*) were identified as being involved in the "Sesquiterpenoid and triterpenoid biosynthesis" pathway, and their transcripts were significantly downregulated in all detected development stages (EGB, GB, GYB, YB and OA) of 'BFN' fruits compared with 'T03' fruits.

Conclusions The findings of this study elucidate a fundamental regulatory mechanism underlying fruit navel formation, and identify two key negative regulators, *MELO3C001812* and *MELO3C004329*, involved in the development of the fruit navel in melon.

Keywords Melon, Fruit navel development, Transcriptome analysis, Expression analysis

Background

Melon is an important horticultural crop, highly valued by consumers for its sweet and flavorful fruit. The flowers of melon are classified into male flowers, female flowers and bisexual flowers [1]. Most melon cultivars exhibit andromonoecy in which bisexual flowers develop into fruits [2]. Under optimal growth conditions, bisexual flowers typically take approximately 5 days to progress from visible buds to full bloom [3]. During anthesis, pollen from male flowers lands on the stigma of the pistil and

*Correspondence:
Wensheng Zhao
zhaowensheng@hebau.edu.cn
[1] College of Horticulture, Hebei Agricultural University, Baoding, Hebei 071000, China
[2] Hebei Key Laboratory of Vegetable Germplasm Innovation and Utilization, Baoding, Hebei 071000, China
[3] Ministry of Education of China-Hebei Province Joint Innovation Center for Efficient Green Vegetable Industry, Baoding, Hebei 071000, China

germinates, the ovule is fertilized in virtue of the growth of pollen tubes [4]. Subsequently, the fruit undergoes rapid growth driven by cell division and expansion. In melons, the morphology of ovary and mature fruit is closely correlated, and the fruit shape is predominantly determined prior to flowering [3].

To date, several quantitative trait loci (QTLs) have been identified as regulators of fruit length (*flqs2.1*, *flqs3b.1*, *flqs6a.1*, *flqs8.1*, *flqs10b.1*), fruit diameter (*fdqs3a.1*, *fdqs12.1*) and fruit shape (*fsqs2.1*, *fsqs8.1*, *fsqs12.1*) in melon [5]. The fruit navel is also a critical component of the exterior quality in melon fruit, and the size of the fruit navel greatly influences consumer preference and its associated economic value. However, the molecular mechanisms underlying fruit navel formation in melon remain largely unexplored.

The fruit navel is the residual trace left after the flower abscises, a prominent scar often appears due to the interplay of genotype, environmental factors and hormonal regulation, and compromises the aesthetic quality of the fruit [6–8]. In tomato, low temperature and growth regulators are important factors contributing to the formation of navel-like scars at the blossom end of fruits [9]. Under low temperature condition, abnormal development of flower organs leads to the production of navel-like scars at the fruit apex [10]. Exogenous application of gibberellic acid (GA_3), N-methatolylphthalamic acid, or 2,3,5-triiodobenzoic acid (TIBA) promotes the formation of large fruit navels in tomato, and the severity of large fruit navel is connected with the plant's developmental stage at the time of induction [9, 11–13]. Specifically, auxin plays a direct role in the development of pointed-tip fruits in tomato. Knockdown of *auxin response factor 7* (*ARF7*) leads to the production of heart-shaped fruits [14]. The *POINTED TIP* (*PT*) gene, which encodes a C2H2-type zinc finger transcription factor, has been demonstrated to suppress the formation of pointed-tip fruits by downregulating the transcription of *FRUTFULL 2* (*FUL2*) and altering auxin transport. Consequently, knockout of *PT* results in the development of pointed-tip fruits in tomato [15]. In melon, low temperature alters the ultrastructure of the phloem, which is responsible for the photoassimilate transport, and inhibits the phloem loading [16, 17]. Additionally, low temperature also results in decreased carbohydrate content in fruits, an altered plant metabolism and a significant loss of productivity [18, 19]. At present, the effects of environmental factors and hormones on the formation of fruit navel in melon remain poorly understood, and the key regulatory genes involved in this process have yet to be identified.

Currently, RNA-seq analysis is widely utilized to identify candidate genes and regulatory pathways associated with key developmental traits in plants. For instance, RNA-seq has been employed to investigate the mechanism underlying the formation of bisexual flowers in melon, revealing that the ethylene signaling pathway plays a crucial role in the initiation of bisexual buds [2]. In this study, the dynamics of fruit navel development were examined using the melon inbred line 'T03' and a big fruit navel mutant 'BFN'. Transcriptome analysis was conducted at the green bud (GB) and ovary at anthesis (OA) stages of 'T03' and 'BFN' fruit navels to explore the molecular mechanisms governing fruit navel development in melon. The results of this study revealed several potential regulators and regulatory networks involved in fruit navel development, and providing valuable insights for improving the exterior quality of melon as well as its consumer appeal.

Methods

Plant materials and growth conditions

This study was conducted from March 2023 to August 2024. The melon inbred line 'T03' (*Cucumis melo* ssp. *agrestis* Jeffrey) and a spontaneous mutant 'BFN' (*Cucumis melo* ssp. *agrestis* Jeffrey) were used for morphological observation, transcriptome sequencing and reverse transcription quantitative polymerase chain reaction (RT-qPCR) analyses. The melon inbred line 'T03' is a widely cultivated variety in Hebei province of China, while 'BFN' is a spontaneous mutant derived from 'T03'. The primary difference between 'T03' and 'BFN' is the size of fruit navel. The melon seedlings were cultivated in the greenhouse of Hebei Agricultural University at 25–28℃/16–19℃ of light/dark of 16/8 h. Standard irrigation and pest management practices were followed throughout the experiment.

RNA extraction and sequencing

Total RNA was extracted from the terminal region of 'T03' and 'BFN' melon fruits at five developmental stages (early green bud (EGB), green bud (GB), green yellow bud (GYB), yellow bud (YB) and ovary at anthesis (OA) stages) using the TianGen Quick RNA Isolation Kit (TianGen Biotech, China). The quality of the isolated total RNA was evaluated by the NanoDrop2000 spectrophotometer (IMPLEN, CA, USA) and 1% RNase-free agarose gel electrophoresis. Samples meeting the quality criteria were selected for further analyses, and the samples at GB and OA stages were chosen to perform RNA-sequencing. Independent samples of melon fruits collected before flowering were used for RNA-seq data validation and expression analyses of several enzyme-coding genes. For RNA sequencing, ten and three fruit navel tissues (indicated by the white frame in Fig. 1A) were pooled to form one biological replicate for the GB and OA stages, respectively. Three biological replicates

were performed for each set (GB-T03, GB-BFN, OA-T03, OA-BFN). RNA-Seq libraries were constructed by Majorbio Bio-Pharm Technology (Shanghai, China) using the Illumina Truseq™ RNA Library Prep Kit following the manufacturer's instructions.

Bioinformatics analysis of RNA-Seq data

The raw paired end-reads were filtered and subjected to quality controlled using fastpusing default parameters [20]. The clean reads were then aligned to the Melon Genome (http://cucurbitgenomics.org/organism/18) in a directed mode using the HISAT2 software [21]. The mapped reads were assembled and spliced by StringTie (http://ccb.jhu.edu/software/stringtie/), and compared with known transcripts to functionally annotate the potential new transcripts [22]. Subsequently, RSEM was employed to quantify the read counts for each gene [23], and the Fragments Per Kilobase of transcript sequence per Millions reads (FPKM) were calculated. Differentially expressed genes (DEGs) between the 'T03' and 'BFN' fruit navels were identified using the DESeq2 R package [24]. The *P*-values were adjusted to control the false discovery rate (FDR) using the Benjamini and Hochberg method. DEGs with a fold change > 2 and an FDR < 0.05 were considered to be differently expressed.

KEGG enrichment analysis of DEGs

The 54 up-regulated genes, 62 down-regulated genes in 'BFN' compared to 'T03' fruits, and all 116 DEGs were subjected to Kyoto Encyclopedia of Genes and Genomes (KEGG) pathway enrichment analysis. The KEGG pathway enrichment was performed by the ClusterProfiler R package [25], with the FDR controlled by the Benjamini and Hochberg method. A KEGG term was considered significantly enriched if its *P*-value was less than 0.05.

Heatmap of DEGs

The heatmap of DEGs was generated by OriginPro 8.0 (OriginLab Corporation, Northampton, MA, USA) based on the read counts. For each gene, the highest and lowest transcript levels were normalized to 1.5 and − 1.5, respectively. The transcript levels in other samples were calculated as the relative values and visualized using a color gradient.

RT-qPCR verification

Total RNA extracted from the fruit navels of 'T03' and 'BFN' melon at the EGB, GB, GYB, YB and OA stages was used to synthesize the cDNA using the FastQuant cDNA Kit (Tiangen Biotech, China). RT-qPCR was performed on a CFX96 Real-time PCR System (Bio-Rad, USA) with SYBR Green PCR master Mix (Applied Biosystems, USA). The melon *CmACTIN* gene (*MELO3C008032*) was used as an internal control. The relative expression level of each gene was calculated by the $2^{-\Delta\Delta Ct}$ method [26]. Gene-specific primers used for RT-qPCR were listed in Table S1.

Statistical analysis

Phenotypic data of the fruit navel in 'T03' and 'BFN' melons were measured from three biological replicates. The Student's *t*-test (*, $P < 0.05$; **, $P < 0.01$) was used to compare the differences in fruit navel diameter between 'BFN' and 'T03' fruits (Fig. 1B). For RT-qPCR assays, three biological replicates and three technical replicates were performed. The Student's *t*-test (*, $P < 0.05$; **, $P < 0.01$) was applied to assess significant differences in transcript levels relative to the GB-T03 sample (Fig. 3), while Duncan's test (lowercase letters, $P < 0.05$) was used to compare the expression differences of five putative enzyme-coding genes in different fruit developmental stages of melon (Fig. 7).

Results

Phenotypic characteristics of fruit navel in 'T03' and 'BFN' melon

Based on corolla color and fruit developmental characteristics, the morphology of the fruit navel was observed at the early green bud (EGB), green bud (GB), green yellow bud (GYB), yellow bud (YB), ovary at anthesis (OA), fruit at 3 days after pollination (DAP), fruit at 7 DAP, fruit at veraison and mature fruit stages (Fig. 1). The melon inbred line 'BFN' is a spontaneous mutant derived from the inbred line 'T03', and exhibits a significantly larger fruit navel compared with 'T03'. During the early green bud stage, no obvious morphological difference was observed in the terminal region of the ovary between 'T03' and 'BFN' melons. However, the diameter of the fruit navel in 'BFN' was notably larger than that in 'T03' (Fig. 1A, B). Starting from the green bud stage, the ovary

(See figure on next page.)

Fig. 1 Phenotypic traits of fruit navel in 'T03' and 'BFN' fruits. **A** Comparison of fruit navels in 'T03' and 'BFN' fruits at the early green bud stage, green bud stage, green-yellow bud stage, yellow bud stage, ovary at anthesis, fruit at 3 days after pollination (DAP) and 7 DAP, fruit at veraison, and mature fruit stages. White frames represent the fruit navel tissues used for RNA-sequencing. **B** Diameter of fruit navel in 'T03' and 'BFN' fruits. Error bars represent ± SD. Asterisks indicate significant differences in the diameter of fruit navel in 'BFN' fruits relative to 'T03' fruits (Student *t*-test: *, $P < 0.05$; **, $P < 0.01$)

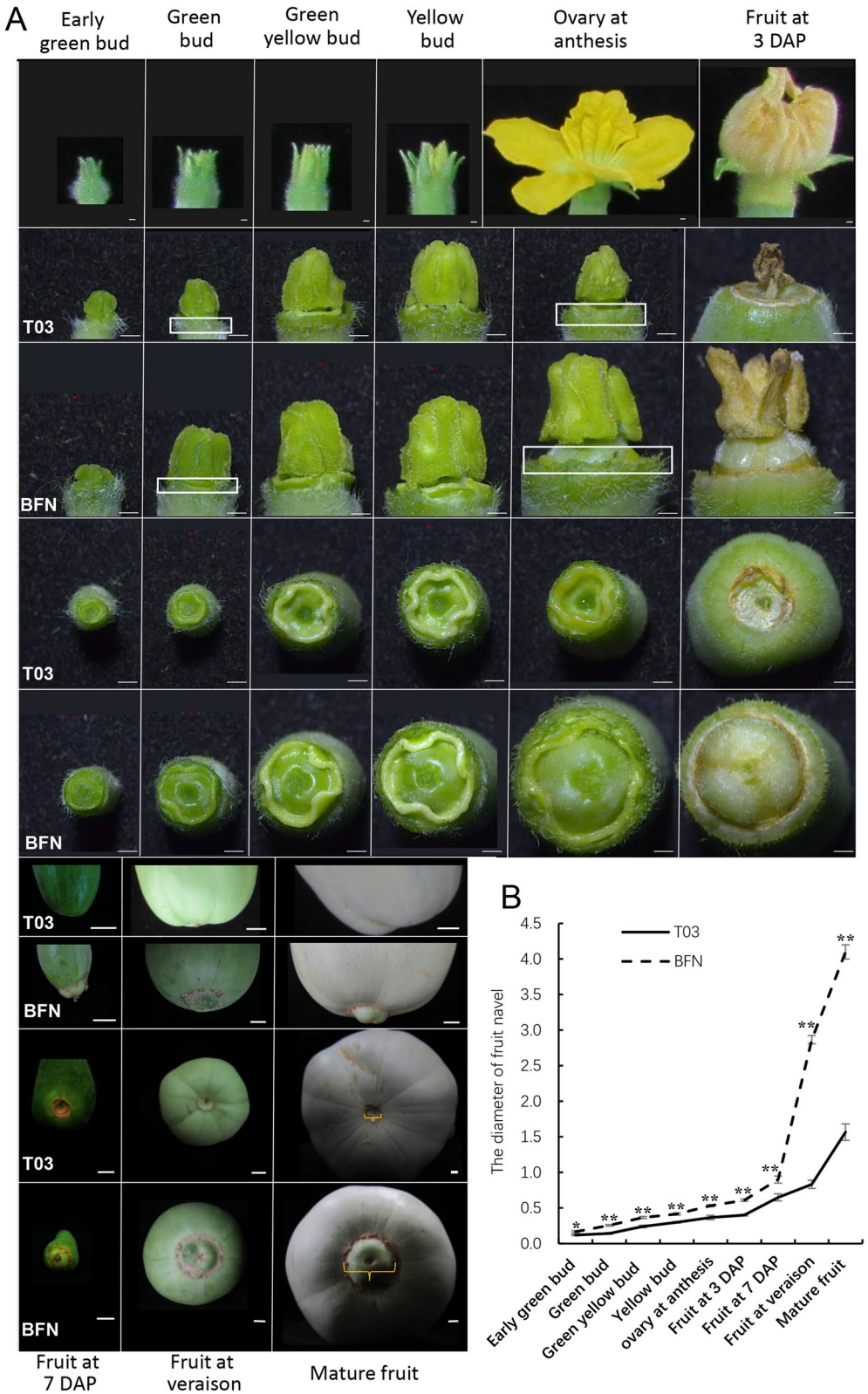

Fig. 1 (See legend on previous page.)

end of 'BFN' began to bulge, whereas the ovary end of 'T03' remained slightly sunken. As a result, a prominent navel formed in 'BFN' fruits, contrasting with the small and smooth navel of 'T03' fruits (Fig. 1A). At the mature fruit stage, the navel diameter of 'T03' fruits was 1.57 cm, while that of 'BFN' fruits reached 4.10 cm (Fig. 1B).

Transcriptomic characteristics of the fruit navel from 'T03' and 'BFN' melons

To investigate the mechanism underlying big fruit navel formation, RNA-seq was conducted on the terminal region of ovaries, specifically the fruit navel region, in 'T03' and 'BFN' melons. The ovary at anthesis (OA) was selected for sampling due to its ease of identification and ability to ensure sampling accuracy. Additionally, transcriptome profiling was performed on the fruit navel of 'BFN' and 'T03' at the green bud (GB) stage, in which the fruit navel exhibits distinct developmental characteristics. Three biological replicates were performed for each set (GB-T03, GB-BFN, OA-T03, OA-BFN), so that a total of 12 libraries were produced (Table. S2). In general, 41.56 to 60.85 million raw reads were generated per sample, and 41.13 to 60.29 million clean reads were mapped to the melon genome after initial data filtering (Table. S2).

The square of Pearson's correlation coefficient (R^2) was closely associated with the developmental stage, and higher R^2 was observed among the three biological replicates within each set compared to those between different groups (Table. S3). Principal component analysis (PCA) revealed clear clustering of samples within the same set, with four distinct clusters corresponding to GB-T03, GB-BFN, OA-T03 and OA-BFN (Fig. 2A). These results indicated that distinct gene expression profiles existed in the fruit navel region of 'BFN' and 'T03' ovaries at the green bud and anthesis stages.

Distinct gene expression profiles contributing the formation of fruit navel

Differential expression genes (DEGs) were identified using a FDR threshold of less than 0.05 and a fold change greater than 2 (Table. S4). During the green bud stage, 186 genes and 394 genes were significantly up-regulated and down-regulated in GB-BFN compared with GB-T03, respectively (Fig. 2B, C). At the anthesis stage, 1404 genes were significantly up-regulated and 478 genes were significantly down-regulated in the fruit navel of 'BFN' compared with that of 'T03' (Fig. 2B, C).

Subsequently, independent samples were collected using the same way as for the RNA-seq analysis, and RT-qPCR was conducted to validate the DEGs results. Eight DEGs were randomly selected, and the expression trends of selected DEGs detected by RT-qPCR were consistent with that of RNA-seq data (Fig. 3). Compared with the ovary of 'T03', three genes were significantly up-regulated and five genes were significantly down-regulated in the 'BFN' melon. The Pearson's correlation coefficient between the RNA-seq and RT-qPCR data was 0.91. These results indicated that the RNA-seq results were highly reliable.

To investigate the mechanism underlying fruit navel formation, DEGs exhibiting consistent expression trends in both the OA and GB stages of 'T03' and 'BFN' melons were selected for further study. A total of 116 DEGs were identified, comprising 54 up-regulated and 62 down-regulated genes in the 'BFN' melon compared with the 'T03' melon during both GB and OA phases (Fig. 2B, C and Fig. 4). Kyoto Encyclopedia of Genes and Genomes (KEGG) enrichment analysis revealed that the 54 up-regulated genes in 'BFN' were significantly enriched in "Biosynthesis of various alkaloids", "Biosynthesis of unsaturated fatty acids", "Isoquinoline alkaloid biosynthesis", "Glycosaminoglycan degradation" pathways. The 62 down-regulated genes were significantly enriched in "Sesquiterpenoid and triterpenoid biosynthesis", "Circadian rhythm—plant" and "Galactose metabolism" pathways (Fig. 5A, B, Table S5). KEGG analysis of the 116 DEGs identified four significantly enriched pathways including "Sesquiterpenoid and triterpenoid biosynthesis", "Circadian rhythm—plant", "Galactose metabolism" and "Biosynthesis of various alkaloids" (Fig. 5C, Table S5). These pathways were hypothesized to play a critical role in the fruit navel development of melon.

Key regulators are involved in the fruit navel formation

Transcription factors play an important role in regulating gene transcription and expression by directly binding to *cis*-acting elements located in the promoter regions of target genes, thereby influencing various growth and developmental processes in plants [27]. There were three (AP2/ERF, MYB and C2H2 types) and eight (AP2/ERF, MADS-box, homeobox domain and bZIP types) transcription factors presented in up-regulated and down-regulated DEGs, and their potential target genes were predicted from the remaining 51 up-regulated and 54 down-regulated DEGs. In the promoter regions of these genes, a total of 13 up-regulated genes were found to contain the GCC (AGCCGCC) or CRT/DRE (A/GCC GAC) *cis*-acting elements, which are recognized by AP2/ERF transcription factors (Fig. 6A, Table S6) [28, 29]. The promoters of 26 and 2 DEGs included the AC (ACC TACC, ACCAACC, ACCTAAC) and elicitor-responsive (AATTGACC) elements, which are recognized by MYB and C2H2 transcription factors, respectively (Fig. 6A, Table S6) [30, 31]. The same way was conducted for the down-regulated DEGs. Specifically, the

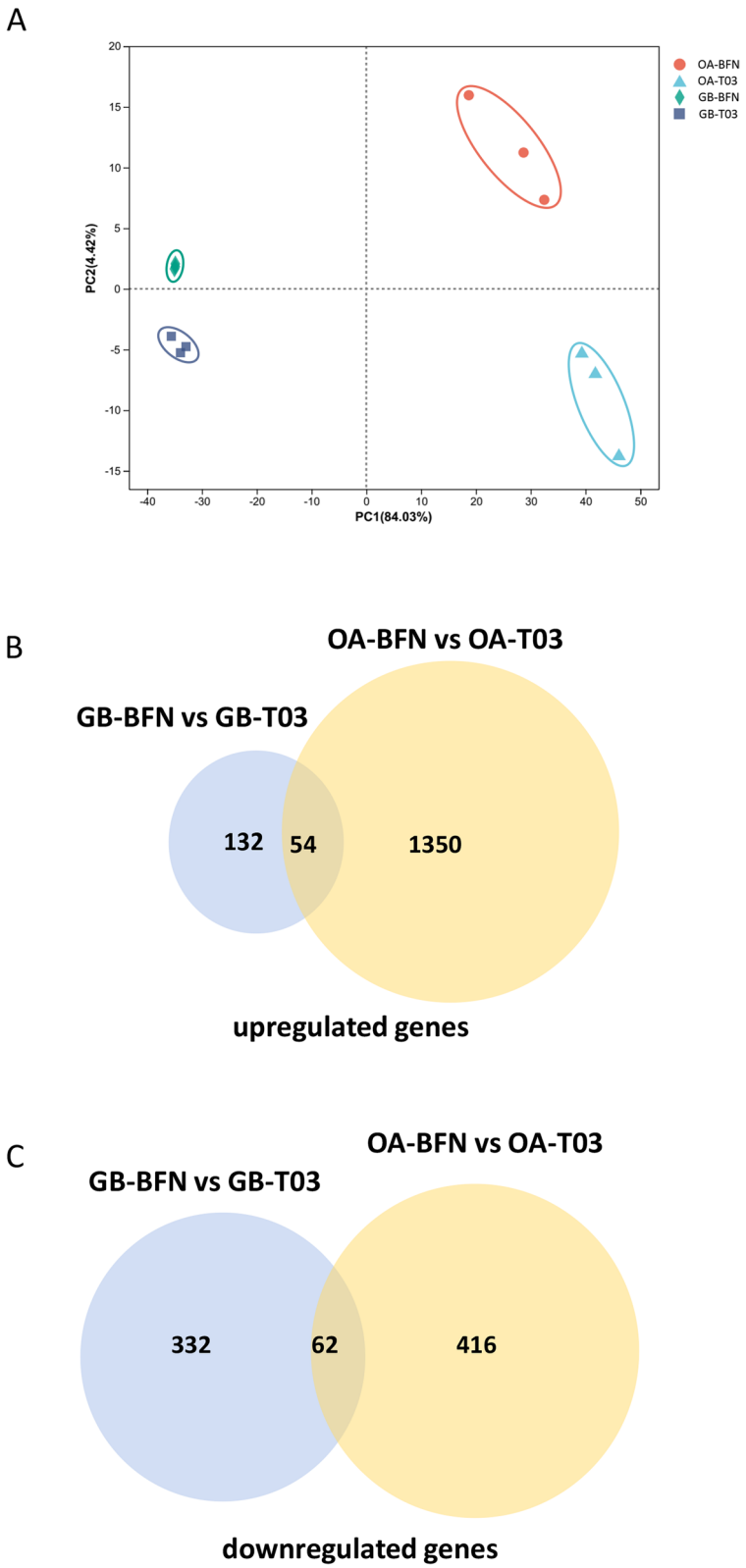

Fig. 2 Transcriptomic characteristics of fruit navel in 'T03' and 'BFN' melon. **A** Principal component analysis (PCA) of GB-T03, GB-BFN, OA-T03 and OA-BFN samples. **B**, **C** Venn diagrams of significantly upregulated (**B**) and downregulated (**C**) genes in 'BFN' fruits compared with 'T03' fruits at GB and OA stages

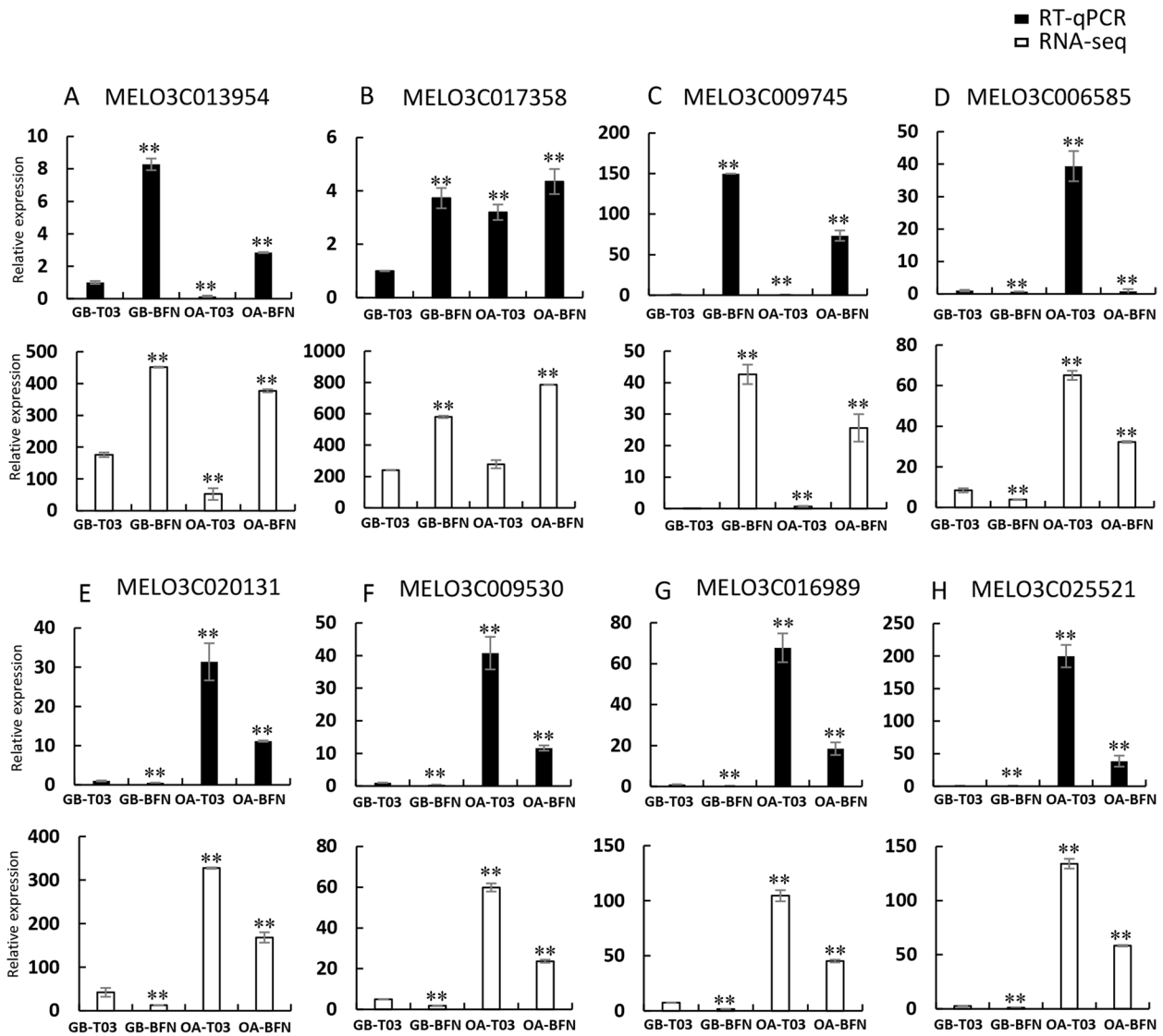

Fig. 3 RT-qPCR validation of RNA-seq data. Three upregulated and five downregulated DEGs identified by RNA-seq were randomly selected for RT-qPCR analyses. The expression trends of the selected DEGs detected by RT-qPCR were consistent with those obtained from RNA-seq. Error bars represent ± SD. Asterisks indicate significant differences in gene expression levels compared with the GB-T03 sample (Student *t*-test: *, $P < 0.05$; **, $P < 0.01$)

promoters of 21, 4, 7 and 46 DEGs contained *cis*-acting elements recognized by AP2/ERF, MADS-box (CArG, CC(A +T-rich)$_6$GG), homeobox domain (HD-ZIP1, CAAT(A/T)ATTG) and bZIP (ACGT, CACGT, CAC GTC, TACGTA) transcription factors, respectively (Fig. 6A, Table S6) [27, 32, 33].

Based on the results of KEGG analyses, two terpene cyclase/mutase family members (*MELO3C001812* and *MELO3C004329*) were identified as participating in the "Sesquiterpenoid and triterpenoid biosynthesis" pathways (Table S5). The putative promoter regions of them contained *cis*-acting elements recognized by bZIP transcription factors. Additionally, the promoter of *MELO3C004329* included *cis*-acting elements for AP2/ERF and homeobox domain transcription factors (Fig. 6B). Within the "Galactose metabolism" pathway, *cis*-acting elements for bZIP and MADS-box transcription factors were identified in putative promoters of *MELO3C002287* (Raffinose synthase) and *MELO3C025521* (Hexosyltransferase), respectively (Fig. 6B, Table S5). Furthermore, a bZIP transcription factor (*MELO3C003686*) and a chalcone synthase (*MELO3C014767*) were implicated in the "Circadian rhythm—plant" pathway (Table S5). The promoter of

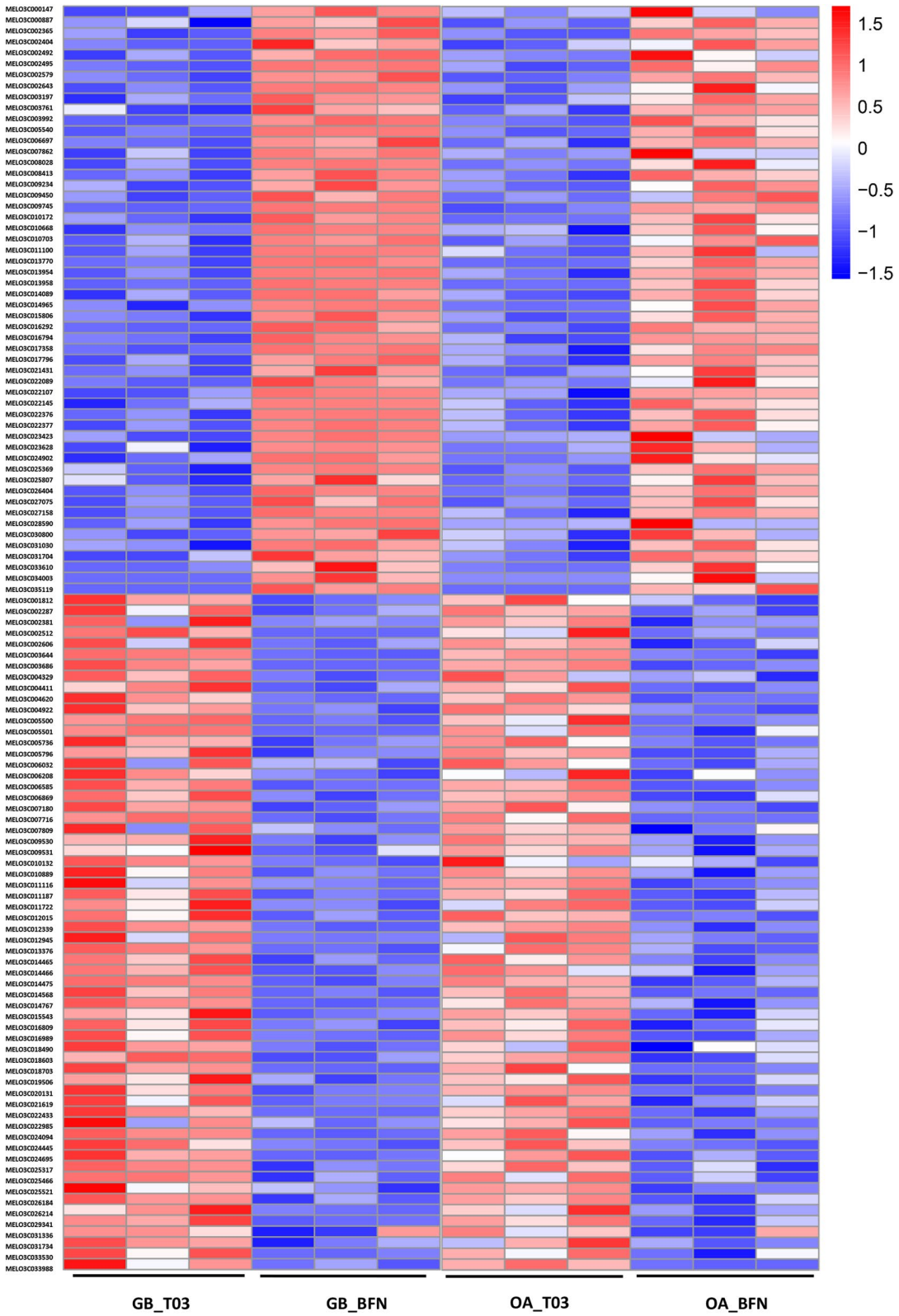

Fig. 4 Expression pattern of 116 DEGs between 'BFN' and 'T03' fruit navels. A total of 54 and 62 genes were significantly upregulated and downregulated, respectively, in both the GB and OA phases of 'BFN' fruits compared with 'T03' fruits. The color blocks represent the relative expression levels of genes, with high and low expression shown in red and blue color, respectively

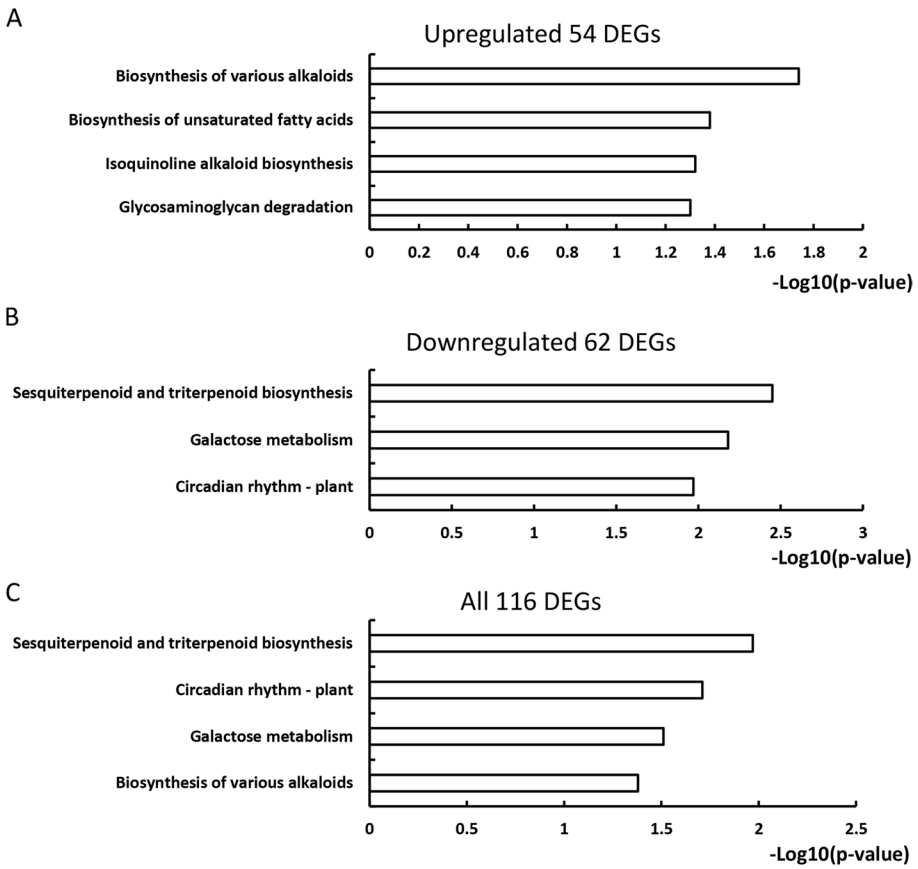

Fig. 5 Significantly enriched ($P < 0.05$) KEGG terms in upregulated (**A**), downregulated (**B**), and all 116 DEGs (**C**) in the fruit navel of 'BFN' fruits compared with 'T03' fruits

MELO3C014767 contained *cis*-acting elements for bZIP, AP2/ERF and homeobox domain transcription factors (Fig. 6B). However, no *cis*-acting elements for AP2/ERF, MYB or C2H2 transcription factors were detected in the promoter region of *MELO3C022377*, a cucumber peeling cupredoxin-like gene involved in the "Biosynthesis of various alkaloids" pathway.

Subsequently, the expression patterns of five putative enzyme-coding genes were analyzed at different fruit developmental stages prior to fertilization. The transcripts of two terpene cyclase/mutase genes (*MELO3C001812* and *MELO3C004329*) were significantly downregulated in all detected stages (EGB, GB, GYB, YB and OA) of 'BFN' fruits compared with 'T03' fruits (Fig. 7A, B). In contrast, *MELO3C002287* exhibited significant upregulation at the YB stage in the fruit navel of 'BFN' compared with 'T03' (Fig. 7C). For *MELO3C025521*, no significant difference in expression levels was observed between 'BFN' and 'T03' fruit navels at the EGB, GB and YB stages (Fig. 7D). Similarly, *MELO3C014767* showed a significant increase in expression at the GYB stage in the fruit navel of 'BFN' compared with 'T03', while no significant difference was detected at the EGB and YB stages (Fig. 7E). These results suggested that *MELO3C001812* and *MELO3C004329*, involved in the "Sesquiterpenoid and triterpenoid biosynthesis" pathway, play a critical role in fruit navel development.

Discussion

Fruits shape and size exhibit significant variation among different melon varieties. Wild melons typically produce small and round fruits, whereas cultivated varieties display a remarkable diversity in fruits morphology due to continuous domestication [3]. The fruit navel, an important component of melon appearance quality, significantly influences consumer preferences. However, the formation process and underlying mechanism of the fruit navel remain poorly understood. In this study, the fruit navel morphologies of the inbred line 'T03' and a spontaneous mutant 'BFN' were compared, and the results showed that the big fruit navel had already formed prior to flowering (Fig. 1). Therefore, the transcriptome profiling was compared on the fruit navel of 'BFN' and 'T03' at green bud (GB) stage and ovary at anthesis (OA) stage

A

Family	Gene ID	Best hits to Arabidopsis	Regulate	FC(GB_BFN/GB_T03)	FC(OA_BFN/OA_T03)	Number of target genes
AP2/ERF	MELO3C025807	AT1G72570/AtAIL1	up	2.340007172	28.172	13
MYB	MELO3C028590	AT1G16490/AtMYB58	up	10.44909963	42.21	26
C2H2	MELO3C027075	AT4G02670/AtIDDI2	up	3.94801083	7.254	2
AP2/ERF	MELO3C019506	AT4G34410/AtERF109	down	0.491772377	0.164230297	21
	MELO3C006869	AT4G25490/AtCBF1	down	0.214987501	0.194018163	
	MELO3C022985	AT3G23240/AtERF1B	down	0.17214353	0.290250562	
	MELO3C015543	AT1G19210/AtERF017	down	0.498910837	0.26093565	
	MELO3C011722	AT2G28550/AtTOE1	down	0.275641453	0.483271551	
MADS-box	MELO3C007716	AT2G22540/AtAGL22	down	0.278076083	0.482543681	4
Homeobox	MELO3C007809	AT4G36740/AtHB40	down	0.043577797	0.426519557	7
bZIP	MELO3C003686	AT5G11260/AtHY5	down	0.348440397	0.477921632	46

B

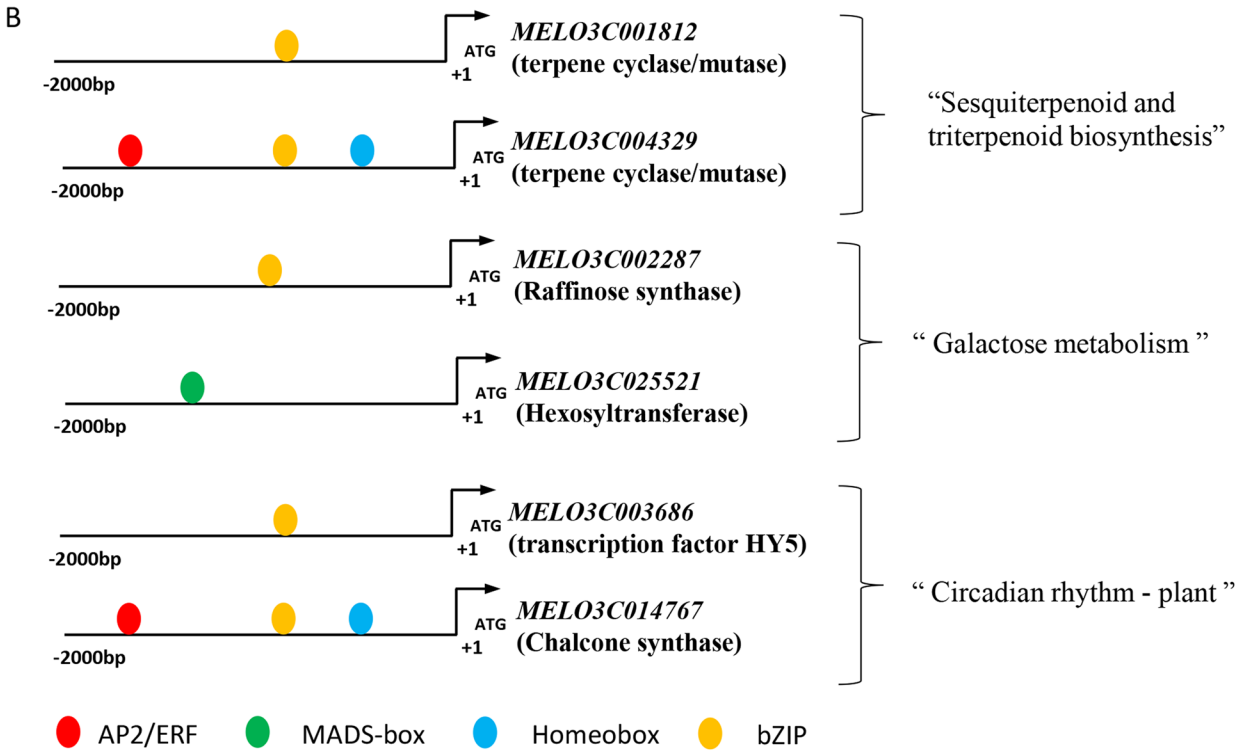

Fig. 6 Identification of key regulators involved in fruit navel formation. **A** Analysis of transcription factors in up-regulated and down-regulated DEGs. Orange and green color represent up-regulated and down-regulated transcription factors, respectively. **B** Promoter analyses of DEGs involved in the "Sesquiterpenoid and triterpenoid biosynthesis", "Galactose metabolism" and "Circadian rhythm—plant" pathways

to investigate the key pathways and regulators involved in fruit navel formation. Through integrated KEGG analysis, promoter analysis and expression analysis, two terpene cyclase/mutase-coding genes (*MELO3C001812* and *MELO3C004329*) involved in the "Sesquiterpenoid and triterpenoid biosynthesis" pathway were identified as being significantly downregulated in 'BFN' fruits compared with 'T03' fruits, and they may play a crucial role in suppressing fruit navel expansion (Fig. 7A, B). Sesquiterpenoid and triterpenoid biosynthesis are known to play vital roles in plant growth, development, and stress resistance [34, 35]. Functional enzymes act as catalysts to ensure efficient material conversion and energy acquisition through activity regulation and specific binding [36]. The findings of this study suggested that terpene cyclase/mutase involved in sesquiterpenoid and triterpenoid biosynthesis may serve as important signaling molecules to regulate the fruit navel development in melon.

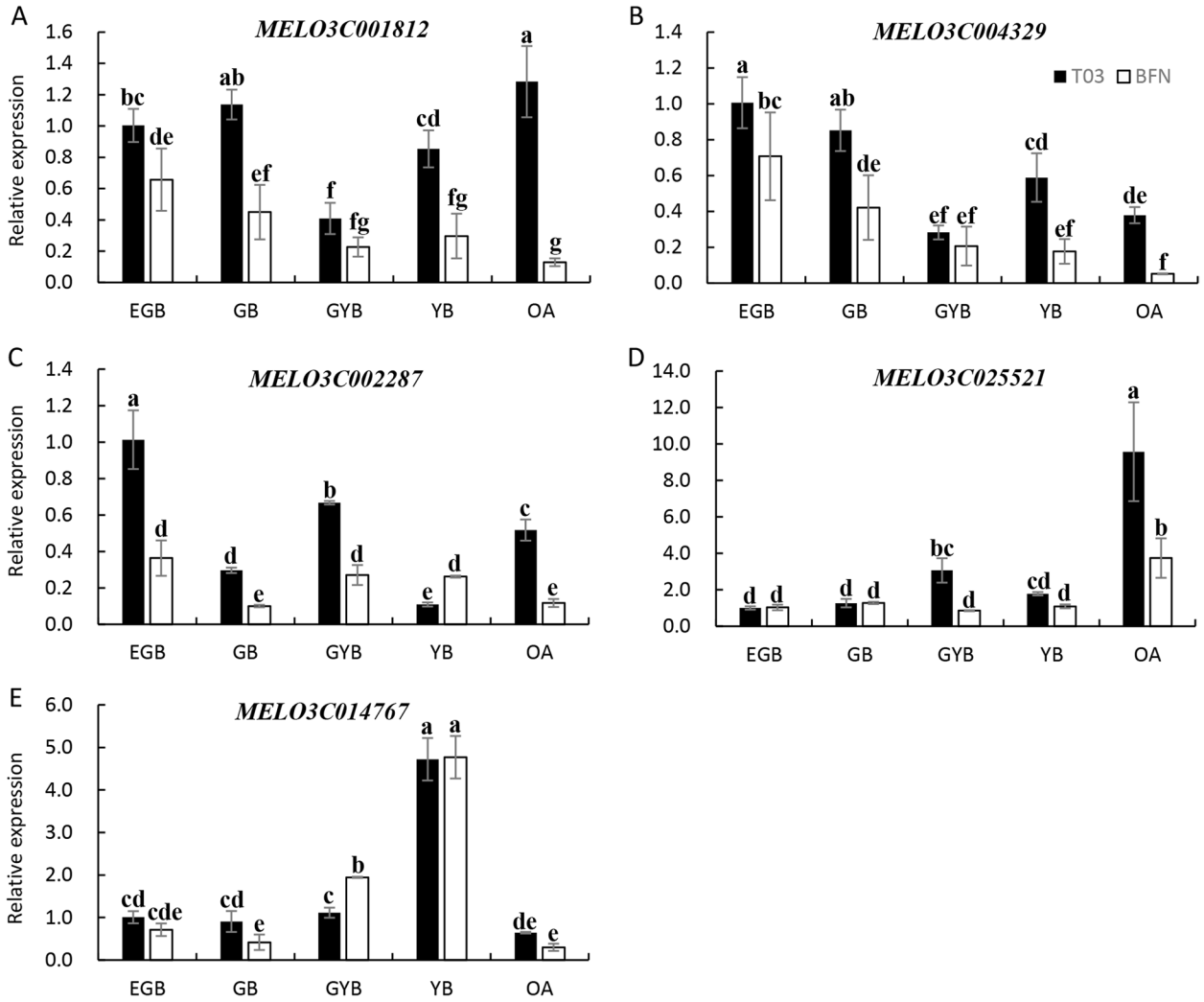

Fig. 7 Expression analyses of five putative enzyme-coding genes identified in the "Sesquiterpenoid and triterpenoid biosynthesis", "Galactose metabolism" and "Circadian rhythm—plant" pathways. RT-qPCR assays were conducted at the early green bud (EGB), green bud (GB), green yellow bud (GYB), yellow bud (YB) and ovary at anthesis (OA) stages. Error bars represent ± SD. Letters above the columns indicate significant differences in transcript levels at $P < 0.05$ (Duncan's test)

Both *MELO3C001812* and *MELO3C004329* showed the highest similarity to *AtLUP4* (lupeol synthase 4 or β-amyrin synthase, *At1G78950*) of Arabidopsis based on BLAST searches conducted in the Arabidopsis Information Resource (http://www.arabidopsis.org/). In Arabidopsis, *AtLUP4* encodes an enzyme responsible for synthesizing the triterpenoid product β-amyrin [37]. In the *gl1* mutant, which is completely devoid of leaf hairs, no pentacyclic triterpenoids were detected, whereas ectopic overexpression of the *AtLUP4* gene resulted in the accumulation of a certain amount of β-amyrin [38]. Triterpenoids are one of the components of surface waxes, which formed a barrier against nonstomatal water loss in many species [39]. Overexpression of *AtLUP4* further negatively affects the intracuticular water barrier of Arabidopsis leaves [38]. However, the function of *LUP4* is just studied in Arabidopsis and remains to be further explored in other higher plants. This study suggested that the *LUP4* homologs in melon (*MELO3C001812* and *MELO3C004329*) may inhibit the expansion of fruit navel, and future studies utilizing the CRISPR/CAS system to generate knockout transgenic lines of *CmLUP4s* could provide valuable insights into the regulatory network underlying fruit navel formation in melon.

In addition to the "Sesquiterpenoid and triterpenoid biosynthesis" pathway, the "Galactose metabolism" and "Circadian rhythm—plant" pathways were also significantly enriched among the down-regulated DEGs

(Fig. 5B, Table S5). Fruit growth and development require the synthesis and metabolism of macronutrients, and galactose is an important component of plant cell wall polysaccharides [40, 41]. In this study, *MELO3C002287* (Raffinose synthase) and *MELO3C025521* (Hexosyltransferase) were identified as participants in the "Galactose metabolism" pathway, and were predicted to be potential target genes of bZIP and MADS-box transcription factors, respectively (Fig. 6B). Circadian rhythm, an intrinsic regulatory mechanism governing plant physiological and biochemical activities, enables plants to optimize photosynthesis, regulate growth, coordinate flowering, and enhance abiotic stress tolerance [42, 43]. In this study, a bZIP transcription factor (*MELO3C003686*) and chalcone synthase (*MELO3C014767*) were found to be involved in the"Circadian rhythm-plant"pathway (Table S5), suggesting their potential involvement in regulating fruit navel development in melon. Future studies will focus on elucidating the specific functions of above-mentioned genes to further clarify the roles of the "Galactose metabolism" and "Circadian rhythm—plant" pathways in fruit navel development of melon.

In addition, transcription factors of the AP2/ERF, MYB, C2H2, MADS-box, homeobox domain and bZIP families were found to be differently expressed during fruit navel development in melon (Fig. 6A). In melon, *CmERF1* has been reported to positively regulate fruit and leaf development, and knockdown of *CmERF1* results in reduced size of ovaries at anthesis, mature fruits and leaves [44]. In citrus, *CsMYB77* negatively regulates fruit ripening and size, and overexpression of *CsMYB77* leads to smaller size and delayed ripening of fruits [45]. In tomato, the C2H2-type zinc-finger transcription factor *PT* inhibits the protuberance of tomato fruit tip by suppressing the transcription of *FRUTFULL 2* (*FUL2*) [15]. In grape, overexpression of the MADS-box gene *VvMADS39* reduces the size of fruit and seed, as well as seed number [46]. In wheat, *HOMEOBOX DOMAIN- 2* (*HB- 2*) is associated with the formation of flower-bearing spikelets and grain protein content [47]. In banana, the bZIP transcription factors *bZIP21* plays a critical role in fruit ripening and ethylene production [48]. These findings indicate that the above-mentioned transcription factors are closely associated with fruit development, and their differential expression in 'BFN' and 'T03' fruits implies their potential involvement in regulating fruit navel development in melon (Fig. 6A). However, the precise functions of these putative regulators in fruit navel formation require further investigation.

In production, a big fruit navel negatively impacts the appearance quality of melons, but this phenomenon is sporadic and unavoidable, potentially resulting from environmental or hormonal variations [9]. In this study, a preliminary mechanism underlying fruit navel formation was explored primarily through RNA-seq and RT-qPCR analyses. In future studies, the function of major regulators of fruit navel development, such as melon *CmLUP4s*, will be explored, and some exogenous growth regulating agents will be applied to reduce or prevent the occurrence of big fruit navel in melon production. In addition, environmental factors influencing the formation of big fruit navels will be investigated to enhance the adaptability of diverse melon varieties, and expand strategies for improving the appearance quality of melon fruits.

Conclusions

In this study, the phenotypic and transcriptomic characteristics of 'T03' and 'BFN' fruits were compared to elucidate the mechanism underlying the fruit navel development of melon. A total of 116 DEGs were identified as being associated with fruit navel development, with significant enrichment in "Sesquiterpenoid and triterpenoid biosynthesis", "Galactose metabolism", "Circadian rhythm—plant" and "Biosynthesis of various alkaloids" pathways. Among these DEGs, three (AP2/ERF, MYB and C2H2 types) and eight (AP2/ERF, MADS-box, homeobox domain and bZIP types) transcription factors were presented in up-regulated and down-regulated DEGs. Notably, *MELO3C001812* and *MELO3C004329*, encoding terpene cyclase/mutase, were significantly downregulated in EGB, GB, GYB, YB and OA stages of 'BFN' fruits compared with 'T03' fruits, suggesting their potential role as key negative regulators in fruit navel development of melon. This study provides a new research direction for improving the appearance quality of melon and holds significant potential for enhancing its economic value.

Supplementary Information

The online version contains supplementary material available at https://doi.org/10.1186/s12870-025-06444-7.

Supplementary Material 1.
Supplementary Material 2.
Supplementary Material 3.
Supplementary Material 4.
Supplementary Material 5.
Supplementary Material 6.

Acknowledgements
Not applicable.

Authors' contributions
T.R. and W.Z. conceived and designed this study, and drafted the manuscript. T.R. and X.S. carried out the sampling and qRT-PCR assays. S.Z. and K.F. analyzed the data. R.Z. and L.N. drew the pictures. All authors read and approved the manuscript.

Funding
This work was supported by the Science and Technology Project of Hebei Education Department (Grant No. BJK2023111), the Hebei Agriculture Research System (Grant No. HBCT2023100208), and the Special Research Foundation of Hebei Agricultural University (Grant No. YJ201837).

Data availability
The sequencing data presented in this study are openly available in Sequence Read Archive (SRA) database at the National Center for Biotechnology Information (https://www.ncbi.nlm.nih.gov/) under accession number PRJNA1191841.

Declarations

Ethics approval and consent to participate
This article does not contain any studies with human participants or animals. The collection materials of the plants, complies the relevant institutional, national, and international guidelines and legislation.

Consent for publication
Not applicable.

Competing interests
The authors declare no competing interests.

Received: 13 February 2025 Accepted: 24 March 2025
Published online: 03 April 2025

References

1. Boualem A, Troadec C, Camps C, Lemhemdi A, Morin H, Sari M-A, et al. A cucurbit androecy gene reveals how unisexual flowers develop and dioecy emerges. Science. 2015;350:688–91.
2. Ge C, Zhao W, Nie L, Niu S, Fang S, Duan Y, et al. Transcriptome profiling reveals the occurrence mechanism of bisexual flowers in melon (Cucumis melo L.). Plant Sci. 2020;301:110694.
3. Monforte AJ, Diaz A, Caño-Delgado A, van der Knaap E. The genetic basis of fruit morphology in horticultural crops: lessons from tomato and melon. J Exp Bot. 2014;65:4625–37.
4. Gillaspy G, Ben-David H, Gruissem W. Fruits: a developmental perspective. Plant Cell. 1993;5:1439–51.
5. Díaz A, Zarouri B, Fergany M, Eduardo I, Alvarez JM, Picó B, et al. Mapping and introgression of QTL involved in fruit shape transgressive segregation into 'piel de sapo' melon (Cucumis melo L.) [corrected]. PLoS One. 2014;9:e104188.
6. Barten JHM, Elkind Y, Scott JW, Vidavski S, Kedar N. Diallel analysis over two environments for blossom-end scar size in tomato. Euphytica. 1992;65:229–37.
7. Elkind Y, Galper OB-O, Vidavski S, Scott JW, Kedar N. Genetic variation and heritability of blossom-end scar size in tomato. Euphytica. 1990;50:241–8.
8. Elkind Y, Galper OB-O, Scott JW, Kedar N. Genotype by environment interaction of tomato blossom-end scar size. Euphytica. 1990;50:91–5.
9. Rylski I. Effect of temperatures and growth regulators on fruit malformation in tomato. Sci Hortic. 1979;10:27–35.
10. Barten JHM, Scott JW, Kedar N, Elkind Y. Low temperatures induce rough blossom-end scarring of tomato fruit during early flower development. jashs. 1992;117:298–303.
11. Hosoki T, Ohta K, Asahira T. Cultivar differences in fruit malformation in tomato and its relationship with nutrient and hormone levels in shoot apices. Engei Gakkai zasshi. 1990;58:971–6.
12. Wien HC, Turner AD. Screening fresh-market tomatoes for susceptibility to catfacing with GA_3 foliar sprays. HortScience. 1994;29:36–7.
13. Wh C, Ta D. Severity of Tomato Blossom-end Scarring is Determined by Plant Age at Induction. J Am Soc Hortic Sci. 1994;119:32–5.
14. de Jong M, Wolters-Arts M, Feron R, Mariani C, Vriezen WH. The *Solanum lycopersicum auxin response factor 7* (*SlARF7*) regulates auxin signaling during tomato fruit set and development. Plant J. 2009;57:160–70.
15. Song J, Shang L, Li C, Wang W, Wang X, Zhang C, et al. Variation in the fruit development gene *POINTED TIP* regulates protuberance of tomato fruit tip. Nat Commun. 2022;13:5940.
16. Hao J, Gu F, Zhu J, Lu S, Liu Y, Li Y, et al. Low Night Temperature Affects the Phloem Ultrastructure of Lateral Branches and Raffinose Family Oligosaccharide (RFO) Accumulation in RFO-Transporting Plant Melon (Cucumis melo L.) during Fruit Expansion. PLoS One. 2016;11:e0160909.
17. Hao JH, Yang R, Fang KF, et al. Low night temperatures inhibit galactinol synthase gene expression and phloem loading in melon leaves during fruit development[J]. Russ J Plant Physiol. 2014;61(2):178–87. https://doi.org/10.1134/S1021443714020058.
18. Hao JH, Li TL, Xu T, Qi HY, Qi MF. Low night-temperatures affect the metabolism of raffinose-family oligosaccharides in melon (Cucumis melo L.) leaves during fruit expansion. The Journal of Horticultural Science and Biotechnology. 2010;85:260–6.
19. Tianlai L, Jinghong H, Zhe D, Yandi W. Effects of night temperature on fruit expansion and polyamine content in Melon. 2009.
20. Chen S, Zhou Y, Chen Y, Gu J. fastp: an ultra-fast all-in-one FASTQ preprocessor. Bioinformatics. 2018;34:i884–90.
21. Kim D, Paggi JM, Park C, Bennett C, Salzberg SL. Graph-based genome alignment and genotyping with HISAT2 and HISAT-genotype. Nat Biotechnol. 2019;37:907–15.
22. Pertea M, Pertea GM, Antonescu CM, Chang T-C, Mendell JT, Salzberg SL. StringTie enables improved reconstruction of a transcriptome from RNA-seq reads. Nat Biotechnol. 2015;33:290–5.
23. Li B, Dewey CN. RSEM: accurate transcript quantification from RNA-Seq data with or without a reference genome. BMC Bioinformatics. 2011;12:323.
24. Love MI, Huber W, Anders S. Moderated estimation of fold change and dispersion for RNA-seq data with DESeq2. Genome Biol. 2014;15:550.
25. Mao X, Cai T, Olyarchuk JG, Wei L. Automated genome annotation and pathway identification using the KEGG Orthology (KO) as a controlled vocabulary. Bioinformatics. 2005;21:3787–93.
26. Man Y-Y, Lv Y-H, Lv H-M, Jiang H, Wang T, Zhang Y-L, et al. *MdDEWAX* decreases plant drought resistance by regulating wax biosynthesis. Plant Physiol Biochem. 2024;206:108288.
27. Conde E, Silva N, Leguilloux M, Bellec A, Rodde N, Aubert J, Manicacci D, et al. A MITE insertion abolishes the *AP3-3* self-maintenance regulatory loop in apetalous flowers of *Nigella damascena*. J Exp Bot. 2023;74:1448–59.
28. Müller M, Munné-Bosch S. Ethylene Response Factors: A Key Regulatory Hub in Hormone and Stress Signaling. Plant Physiol. 2015;169:32–41.
29. Cheng M-C, Liao P-M, Kuo W-W, Lin T-P. The *Arabidopsis ETHYLENE RESPONSE FACTOR1* regulates abiotic stress-responsive gene expression by binding to different *cis*-acting elements in response to different stress signals. Plant Physiol. 2013;162:1566–82.
30. Gao Y, Jia S, Wang C, Wang F, Wang F, Zhao K. BjMYB1, a transcription factor implicated in plant defence through activating *BjCHI1* chitinase expression by binding to a W-box-like element. J Exp Bot. 2016;67:4647–58.
31. de Pater S, Greco V, Pham K, Memelink J, Kijne J. Characterization of a zinc-dependent transcriptional activator from Arabidopsis. Nucleic Acids Res. 1996;24:4624–31.
32. Izawa T, Foster R, Chua NH. Plant bZIP protein DNA binding specificity. J Mol Biol. 1993;230:1131–44.
33. Ariel FD, Manavella PA, Dezar CA, Chan RL. The true story of the HD-Zip family. Trends Plant Sci. 2007;12:419–26.
34. Khurshid U, Ahmad S, Saleem H, Lodhi AH, Pervaiz I, Khan MA, et al. Multifaced Assessment of Antioxidant Power, Phytochemical Metabolomics, In-Vitro Biological Potential and In-Silico Studies of Neurada procumbens L.: An Important Medicinal Plant. Molecules. 2022;27:5849.
35. Xu J, Hu Z, He H, Ou X, Yang Y, Xiao C, et al. Transcriptome analysis reveals that jasmonic acid biosynthesis and signaling is associated with the biosynthesis of asperosaponin VI in *Dipsacus asperoides*. Front Plant Sci. 2022;13:1022075.
36. Bourlieu C, Astruc T, Barbe S, Berrin J-G, Bonnin E, Boutrou R, et al. Enzymes to unravel bioproducts architecture. Biotechnol Adv. 2020;41:107546.
37. Shibuya M, Katsube Y, Otsuka M, Zhang H, Tansakul P, Xiang T, et al. Identification of a product specific beta-amyrin synthase from *Arabidopsis thaliana*. Plant Physiol Biochem. 2009;47:26–30.

38. Buschhaus C, Jetter R. Composition and physiological function of the wax layers coating Arabidopsis leaves: β-amyrin negatively affects the intracuticular water barrier. Plant Physiol. 2012;160:1120–9.
39. Riederer M, Schreiber L. Protecting against water loss: analysis of the barrier properties of plant cuticles. J Exp Bot. 2001;52:2023–32.
40. Gross KC, Pharr DM. A Potential Pathway for Galactose Metabolism in Cucumis sativus L., A Stachyose Transporting Species. Plant Physiol. 1982;69:117–21.
41. Zhang H, Zhang K, Zhao X, Bi M, Liu Y, Wang S, et al. Galactinol synthase 2 influences the metabolism of chlorophyll, carotenoids, and ethylene in tomato fruits. J Exp Bot. 2024;75:3337–50.
42. Okada M, Yang Z, Mas P. Circadian autonomy and rhythmic precision of the Arabidopsis female reproductive organ. Dev Cell. 2022;57:2168-2180.e4.
43. Venkat A, Muneer S. Role of Circadian Rhythms in Major Plant Metabolic and Signaling Pathways. Front Plant Sci. 2022;13:836244.
44. Sun Y, Yang H, Ren T, Zhao J, Lang X, Nie L, et al. CmERF1 acts as a positive regulator of fruits and leaves growth in melon (Cucumis melo L.). Plant Mol Biol. 2024;114:70.
45. Zhang L, Xu Y, Li Y, Zheng S, Zhao Z, Chen M, et al. Transcription factor *CsMYB77* negatively regulates fruit ripening and fruit size in citrus. Plant Physiol. 2024;194:867–83.
46. Zhang S, Yao J, Wang L, Wu N, van Nocker S, Li Z, et al. Role of grapevine *SEPALLATA*-related MADS-box gene *VvMADS39* in flower and ovule development. Plant J. 2022;111:1565–79.
47. Dixon LE, Pasquariello M, Badgami R, Levin KA, Poschet G, Ng PQ, et al. MicroRNA-resistant alleles of HOMEOBOX DOMAIN-2 modify inflorescence branching and increase grain protein content of wheat. Sci Adv. 2022;8:eabn5907.
48. Wu C-J, Shan W, Liu X-C, Zhu L-S, Wei W, Yang Y-Y, et al. Phosphorylation of transcription factor *bZIP21* by MAP kinase *MPK6-3* enhances banana fruit ripening. Plant Physiol. 2022;188:1665–85.

Publisher's Note